Ultrasound in Med. & Biol., Vol. 32, No. 2, pp. 237–247, 2006

0301-5629/06/$–see front matter

ELSEVIER

doi:10.1016/j.ultrasmedbio.2005.10.007

● *Original Contribution*

BREAST ULTRASOUND IMAGE ENHANCEMENT USING FUZZY LOGIC

YANHUI GUO,* H. D. CHENG,† JIANHUA HUANG,* JIAWEI TIAN,‡ WEI ZHAO,* LITAO SUN,‡ and YANXIN SU‡

*School of Computer Science and Technology, Harbin Institute of Technology, Harbin, China; †Department of Computer Science, Utah State University, Logan, UT, USA; ‡Second Affiliated Hospital of Harbin Medical University, Harbin, China

(*Received* 14 *June* 2005, *revised* 5 *October* 2005, *in final form* 13 *October* 2005)

Abstract—Breast cancer is still a serious disease in the world. Early detection is very essential for breast cancer prevention and diagnosis. Breast ultrasound (US) imaging has been proven to be a valuable adjunct to mammography in the detection and classification of breast lesions. Because of the fuzzy and noisy nature of the US images and the low contrast between the breast cancer and tissue, it is difficult to provide an accurate and effective diagnosis. This paper presents a novel algorithm based on fuzzy logic that uses both the global and local information and has the ability to enhance the fine details of the US images while avoiding noise amplification and overenhancement. We normalize the images and then fuzzify the normalized images based on the maximum entropy principle. Edge and textural information are extracted to describe the lesion features and the scattering phenomenon of US images and the contrast ratio measuring the degree of enhancement is computed and modified. The defuzzification process is used to obtain the enhanced US images. To demonstrate the performance of the proposed approach, the algorithm was tested on 86 breast US images. Experimental results confirm that the proposed method can effectively enhance the details of the breast lesions without overenhancement or underenhancement. (E-mail: hengda.cheng@usu.edu) **© 2006 World Federation for Ultrasound in Medicine & Biology.**

Key Words: **Contrast enhancement, Fuzzy logic, Texture analysis, Maximum entropy principle, Breast ultrasound image.**

INTRODUCTION

Breast cancer is still one of the most common cancers and a serious disease among women in the world. Because the causes of this disease still remain unknown, early detection is essential for diagnosis and it makes the treatment more effective in reducing the mortality and cost.

Mammography and ultrasonography have been preferred methods for breast cancer detection. Mammography is very sensitive, but not specific, for detecting breast cancer (Joseph et al. 1999). As a result, approximately 65% of the cases referred for surgical biopsy are actually benign lesions (Kopans 1992; Knutzen and Gisvold 1993). Mammography also has limitations for cancer detection in dense breast tissue of young patients. Currently, breast ultrasound (US) imaging is a valuable adjunct to mammography in the early detection and classification of breast lesions (Drukker et al. 2004). Sonography was more effective for women younger than 35 years old (Bassett et al. 1991). The results (Laine et al. 1995) suggest that the more dense the breast parenchyma, the higher is the detection accuracy of malignant tumors using US. The accuracy rate of breast US imaging has been reported to be 96 to 100% in the diagnosis of simple benign cysts (Jackson 1990). Breast US examination has played a more and more significant role in detecting breast cancers because of the fact that sonography has the ability to show masses obscured mammographically by dense tissue and has no ionizing radiation and because of its low cost and portability (Drukker et al. 2004).

Image enhancement is used to improve the quality of the image and to correct deficiencies of the contrast. Many algorithms have been proposed to enhance images. An automatic image-enhancement algorithm driven by an evolutionary optimization process was studied (Munteanu and Rosa 2004) that proposed an objective criterion and used an evolutionary algorithm as a global search strategy for the best enhancement. However, the

Address correspondence to: Prof. H. D. Cheng, Department of Computer Science, Utah State University, Logan, UT 84322-4205 USA. E-mail: hengda.cheng@usu.edu

evolutionary algorithm requires making a series of trial enhancements to find the final result and the algorithm has quite high computational complexity. That paper only compared the results with those of classical linear contrast stretching and histogram equalization techniques that are quite old. One method generalized the linear scale spaces in the complex domain by combining the diffusion equation with the free Schrödinger equation for image enhancement and denoising (Gilboa et al. 2004). Two examples of nonlinear complex processes were developed; a regularized shock filter for image enhancement and a ramp-preserving denoising process. However, they did not discuss underenhancement and overenhancement. Three quantitative measures of contrast enhancement of mammographic images in a computer-aided system were proposed (Singh and Bovis 2005) that can be used for selecting the best-suited image enhancement on a per mammogram basis. However, the method was only tested on six enhancement algorithms.

It is well known that breast US images have some degree of fuzziness, such as indistinct cyst borders, ill-defined mass shapes and different tumor densities. Some nonlinear filters were used to enhance the US images. A morphologic method, alternating sequential filter, to enhance US images that is an iterative application of openings and closings with structuring elements of increasing sizes, was studied (Tsubai et al. 2000). No objective method for determining the number of iterations was supplied and it is difficult to enhance the image and remove noise at the same time. A nonlinear enhancing filter is based on sorting the elements in a moving window and extracting statistical characteristics from them (Lee et al. 2001). The filter compared the statistical values of the front and back points with those of the center point in the window and estimated the output using the compared result. However, the enhancement was affected by the size of the filters and how to determine the size and number of filters was not discussed in detail. Many nonlinear or linear map functions are used to enhance the contrast of US image in space or other domains. The grey-level mapping technique was applied to enhance the US images having different levels of contrast and brightness (Saim et al. 2000). Grey-level mapping is a technique to map the input grey levels (low and high) to the stretched output grey levels (bottom and top) observed in a look-up table. The mapping function is an exponential function and its parameter is a constant that cannot vary with different images. A nonlinear algorithm was studied for contrast enhancement, which is accomplished *via* nonlinear stretching followed by hard thresholding of wavelet coefficients within midrange spatial frequency levels (Zhou et al. 2002). But the selection of the threshold is subjective and the image enhancement is highly dependent on the value of the threshold.

An algorithm uses line segments (called "sticks") in different angular orientations as templates and selects the orientation at each point that is most likely to represent a line in the image to improve edge information, making the line segments more suitable for edge detection and for US image enhancement (Pathak et al. 2000; Pathak and Kim 2000; Abolmaesumi and Sirouspour 2004; Awad et al. 2003). However, the algorithm only enhances the edge information and the features inside the tissues and lesions are not affected.

Fuzzy set theory is used to enhance US images (Li et al. 2003, 2004). The image is transformed into fuzzy domain using membership function and then the membership is enhanced by an iterative four-segment function. However, the rules of the iterative four-segment function and the iteration time are fixed and subjective. Also, the method only uses global features that cannot reflect the local contrast change. A new fuzzy logic filter for image enhancement was reported (Farbiz et al. 2000) that was based on fuzzy-logic control, with the ability to remove impulsive noise and smooth Gaussian noise while simultaneously preserving edges and image details. However, how to deal with overenhancement and underenhancement was not discussed.

A statistical model using tissue properties and intensity inhomogeneities in US was presented and used in contrast enhancement and image segmentation and the maximum *a posteriori* principle was used to correct tissue intensity and to conduct contrast enhancement of breast US images (Xiao et al. 2000). The methods only modified the distribution of the intensities and did not pay much attention to the features of tumors and tissues.

Among the early indicators of breast cancers, masses and microcalcifications are the primary features (Lanyi 1986) that are very important visual features of early cancers found by radiologists (Mclelland 1990). Unfortunately, at the early stage of breast cancer, the inside structure and border of masses of US images are very subtle and varied in appearance; hence, it makes the diagnosis very difficult. The difference between the suspicious areas and normal tissues can be very slight. Breast US image enhancement, especially for the images of dense breasts, is exceedingly important for both the doctors and computer-aided diagnosis systems. After enhancement, more useful information can be extracted.

In this paper, we propose a novel contrast-enhancement algorithm based on fuzzy logic and the characteristics of breast US images. The maximum fuzzy entropy principle is used to map the original image, then the characteristics of the US image are taken into account. Specifically, the edge and textural information is extracted to evaluate the lesion features and the scattering phenomenon of US images and the local information is used to define the enhancement criterion. Finally, the

algorithm enhances the details and lesion features using the local fuzzy information.

The paper is organized as follows. In the next section, the proposed method is presented in detail. Experiments are then discussed to demonstrate the performance of the algorithm. Finally, the conclusions are drawn.

PROPOSED APPROACH

The proposed method consists of the following steps; image normalization, image fuzzification, edge information extraction, textural information extraction and contrast enhancement.

Normalization

The distribution of grey levels of breast US images may vary largely and the ranges of the intensities are quite narrow. Normalization is a necessary step and we normalize the US images by mapping the intensity levels into the range $[g_{\min}, g_{\max}]$:

$$g(i,\ j) = g_{\min} + \frac{(g_{\max} - g_{\min}) \times (g_o(i,\ j) - g_{o\min})}{(g_{o\max} - g_{o\min})}, \quad (1)$$

where $g_{o\min}$ and $g_{o\max}$ are the minimum and maximum intensity levels of the original image, $g_{\min}$ and $g_{\max}$ are the minimum and maximum intensity levels of the normalized image and $g_o(i, j)$ and $g(i, j)$ are the grey levels of pixel (i, j) before and after normalization. In our experiments, $g_{\min} = 0$ and $g_{\max} = 255$.

Fuzzification

To apply fuzzy logic to deal with the fuzzy nature of breast US images, we need to find a suitable membership function, which maps all the elements of a set into the real numbers in [0, 1]. The most-commonly used membership function for a grey-level image is the standard S function (Pal et al. 1986):

$$S(g; x,\ y,\ z) = \begin{cases} 0 & g \le x \\ \dfrac{(g-x)^2}{(y-x)(z-x)} & x \le g \le y \\ 1 - \dfrac{(g-z)^2}{(z-y)(z-x)} & y \le g \le z \\ 1 & g \ge z \end{cases} \quad (2)$$

The values of the function represent the brightness degrees of the pixel intensities. It is depicted in Fig. 1.

In breast US images, the mass areas, breast structure areas, etc. belong to the object group and other regions belong to the background. In eqn (2), the selection of the middle point y could be determined as an object-background classification problem (Sahoo et al. 1988) using the entropy principle (Cheng et al. 1998; Kapur et al. 1985). Let p_i be the original probability distribution of grey levels i, $i = 1,2, \ldots .. . ., N$. The output distributions of intensity levels are as follows. The entropies of the distributions below and above than the threshold t can be defined as $H_l(t)$ and $H_g(t)$, respectively:

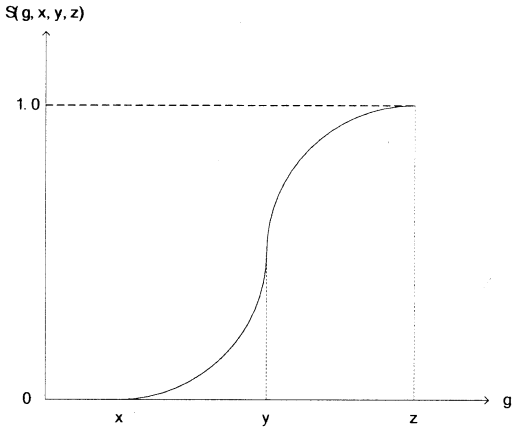

Fig. 1. The S function.

$$H_l(t) = -\sum_{i=1}^{l} \frac{p_i}{P_l} \ln \frac{p_i}{P_l} \quad (3)$$

$$H_g(t) = -\sum_{i=l+1}^{N} \frac{p_i}{1-P_l} \ln \frac{p_i}{1-P_l} \quad (4)$$

$$P_l = \sum_{i=1}^{l} p_i \quad (5)$$

where t is the threshold and N is the maximum intensity of the image.

The maximum entropy can be obtained by:

$$t^* = \underset{i=1}{\overset{N}{Arg\ \max}} \{H_l(t) + H_g(t)\}, \quad (6)$$

where i^* is the optimal threshold that is used as the middle point of the S function. The US image is, thus, transformed from the intensity domain into the fuzzy domain using the S function.

$$\mu(i,\ j) = S(g(i,\ j); x,\ t^*,\ z) \quad (7)$$

$$h_g(m) = \sum_{m=0}^{\substack{0 \le j \le H-1 \\ \max\ (g(i,j)) \\ 0 \le i \le H-1}} \delta(g(i,\ j) - m) \quad (8)$$

$$\delta(t) = \begin{cases} 1 & t = 0 \\ 0 & otherwise \end{cases}, \quad (9)$$

where $g(i, j)$ is the intensity of pixel (i, j), $h_g(m)$ is the grey-level histogram, m is the grey level and H and W are the height and width of the image. The values of x and z are the grey levels corresponding to the first peak and last peak of $h_g(m)$, respectively. If $(h_g(n) > h_g(n-1)) \cap (h_g(n) > h_g(n+1))$, then $h_g(n)$ is a peak.

Edge information extraction

Among the early indicators of breast cancer, the mass shape and margin and the membrane smoothness are the primary features. To obtain the edge feature, an edge operator is applied to the fuzzified image and then the value of the edge information is normalized:

$$e_\mu(i, j) = \frac{\delta_\mu(i, j) - \delta_{\mu\min}}{\delta_{\mu\max} - \delta_{\mu\min}} \quad (10)$$

where $\delta_\mu(i, j)$ is the edge value computed by using Sobel operator (Parker 1997) because of its simplicity and high speed, $\delta_{\mu\max} = \max(\delta_\mu(i, j)$ and $\delta_{\mu\min} = \min(\delta_\mu(i, j))$ $(0 \le i \le H - 1, 0 \le j \le W - 1)$.

Texture information extraction

There are many methods for describing the texture features. A method (Sivaramakrishna et al. 2002) computed 28 descriptors at 5 different-sized neighborhoods to make a total of 140 descriptors. Another algorithm (Wu et al. 1992) studied the classification of ultrasonic liver images by using some texture features; there were the spatial grey-level difference statistics, the Fourier power spectrum, the grey-level difference statistics and the Laws texture energy measures (Laws 1979).

The scattering phenomenon is the main characteristic of US images and occurs when tissues are rough or smaller than the scale of the wavelength. Many small lesion and tissue features can be gained from scattering on US images. In this paper, the Laws (1979) texture energy measures are used to determine the textural properties of regions-of-interest (ROIs) in the fuzzy domain. Four masks are used to depict the edge and spot features of scattering, which are derived from the three simple vectors, $L5 = (1,4,6,4,1)$, $E5 = (-1,-2,0,2,1)$ and $S5 = (-1,0,2,0,-1)$.

$$L5^T \times E5 = \begin{bmatrix} -1 & -2 & 0 & 2 & 1 \\ -4 & -8 & 0 & 8 & 4 \\ -6 & -12 & 0 & 12 & 6 \\ -4 & -8 & 0 & 8 & 4 \\ -1 & -2 & 0 & 2 & 1 \end{bmatrix} \quad (M1)$$

$$L5^T \times S5 = \begin{bmatrix} -1 & 0 & 2 & 0 & -1 \\ -4 & 0 & 8 & 0 & -4 \\ -6 & 0 & 12 & 0 & -6 \\ -4 & 0 & 8 & 0 & -4 \\ -1 & 0 & 2 & 0 & -1 \end{bmatrix} \quad (M2)$$

$$E5^T \times L5 = \begin{bmatrix} -1 & -4 & -6 & -4 & -1 \\ -2 & -8 & -12 & -8 & -2 \\ 0 & 0 & 0 & 0 & 0 \\ 2 & 8 & 12 & 8 & 2 \\ 1 & 4 & 6 & 4 & 1 \end{bmatrix} \quad (M3)$$

$$S5^T \times L5 = \begin{bmatrix} -1 & -4 & -6 & -4 & -1 \\ 0 & 0 & 0 & 0 & 0 \\ 2 & 8 & 12 & 8 & 2 \\ 0 & 0 & 0 & 0 & 0 \\ 1 & -4 & -6 & -4 & -1 \end{bmatrix} \quad (M4)$$

The texture value of pixel (i, j), $f_\mu(i, j)$, is derived:

$$f_\mu(i,j) = \frac{abs\left(f_{\mu L5^T \times E5}(i,j)\right)}{f_{\mu L5^T \times E5_{\max}}} \times \frac{abs\left(f_{\mu L5^T \times S5}(i,j)\right)}{f_{\mu L5^T \times S5_{\max}}} \times \frac{abs\left(f_{\mu E5^T \times L5}(i,j)\right)}{f_{\mu E5^T \times L5_{\max}}} \times \frac{abs\left(f_{\mu S5^T \times L5}(i,j)\right)}{f_{\mu S5^T \times L5_{\max}}} \quad (11)$$

where $f_{\mu L5^T} \times E5(i, j)$, $f_{\mu L5^T} \times S5(i, j)$, $f_{\mu E5^T} \times L5(i, j)$ and $f_{\mu\ S5^T} \times L5(i, j)$ are the convoluted results of the $\mu(i, j)$ with the four masks and $f_{\mu L5^T} \times E5\max = \max(abs(f_{\mu L5^T} \times E5(i, j)))$, $f_{\mu L5^T} \times S5\max = \max(absf_{\mu E5^L} \times S5(i, j)))$, $f_{\mu E5^T} \times L5\max = \max(absf_{\mu E5^T} \times L5(i, j)))$ and $f_{\mu S5^T} \times L5\max = \max(absf_{\mu S5^T} \times L5(i, j)))$, respectively $(0 \le i \le H - 1, 0 \le j \le W - 1)$.

Contrast enhancement

Many definitions of contrast have been studied (Hall 1979). Usually, the contrast, C, is defined as (Morrow et al. 1992):

$$C = \frac{(f - b)}{(f + b)}, \quad (12)$$

where f and b are the maximum intensity and the minimum intensity of the image, respectively.

The contrast is used to measure the relation between the current pixel and the neighboring pixels in a window and the value of membership $\mu(i, j)$ should be compared with the local mean value $\bar{\mu}_w(i, j)$. To measure the local changes of the edge and texture information in the fuzzy domain, the local mean value $\bar{\mu}_w(i, j)$ should not be calculated by only using the membership in a window,

but also by using the values of $f_\mu(i, j)$ and $e_\mu(i, j)$. Therefore, we will use the following contrast definition:

$$C_\mu(i,j) = \left|\mu(i, j) - \overline{\mu}_w(i, j)\right| / \left|\mu(i, j) + \overline{\mu}_w(i, j)\right| \tag{13}$$

$$\overline{\mu}_w(i, j) = \sum_{m=i-(w-1)/2}^{i+(w-1)/2} \sum_{n=j-(w-1)/2}^{j+(w-1)/2} (\mu(m, n) \times f_\mu(m, n) \times e_\mu(m, n) \Big/ \sum_{m=i-(w-1)/2}^{i+(w-1)/2} \sum_{n=j-(w-1)/2}^{j+(w-1)/2} f_\mu(m, n) \times e_\mu(m, n), \tag{14}$$

where $\bar{\mu}_w(i, j)$ is the local mean of a window whose size is $w \times w$ and centered at location (i, j).

The new contrast C' can be obtained by using a nonlinear function of C or an empirically determined relationship between C' and C. Previously, analytic functions (square root, exponential and logarithmic) were used (Rangayyan and Rguyen 1986; Dhawan et al. 1986). It has been found that an empirically formed chart or plot defining the relationship between C' and C gives better results (Morrow et al. 1992).

An exponential function $k(i, j)$ transforms C_μ into C'_μ, which especially boosts the perceptibility of regions with low contrast while not affecting high-contrast regions.

$$C'_\mu(i,j) = \left(C_\mu(i,j)\right)^{k(i,j)}, \tag{15}$$

where $k(i, j)$ is the local contrast amplification constant of pixel (i, j). It significantly affects the degree of the contrast enhancement. $k(i, j)$ should be determined automatically according to the nature of the original image. How to determine the value of $k(i, j)$ will be discussed later.

After the contrast is enhanced, the modified membership value $\mu'(i, j)$ of pixel (i, j) can be obtained by the following equation:

$$\mu'(i,j) = \begin{cases} \overline{\mu}_w(i,j)\left(1 + C'_\mu(i, j)\right) / \left(1 - C'_\mu(i, j)\right) & \mu(i,j) \geq \overline{\mu}_w(i,j) \\ \overline{\mu}_w(i,j)\left(1 - C'_\mu(i, j)\right) / \left(1 + C'_\mu(i, j)\right) & \mu(i,j) < \overline{\mu}_w(i,j) \end{cases}. \tag{16}$$

Defuzzification

The enhanced intensity of pixel (i, j) can be obtained by using the inverse function $S^{-1}(\mu'(i, j);x,y,z)$.

$$g'(i, j) = S^{-1}\left(\mu'(i, j); x, y, z\right) = \begin{cases} g_{\min} + \dfrac{g_{\max} - g_{\min}}{z - x}\sqrt{\mu'(i, j) \times (y - x)(z - x)} & 0 \leq \mu'(i, j) \leq \dfrac{(y - x)}{(z - x)} \\ g_{\min} + \dfrac{g_{\max} - g_{\min}}{z - x}\left(z - x - \sqrt{\left(1 - \mu'(i, j)\right) \times (z - y)(z - x)}\right) & \dfrac{(y - x)}{(z - x)} < \mu'(i, j) \leq 1 \end{cases}, \tag{17}$$

where $g_{\min}$ and $g_{\max}$ are the minimum grey level and maximum grey level after the enhancement.

Determine the amplification exponent k(i, j)

We need to calculate the local fuzzy entropy $En(i, j)$ at pixel (i, j):

$$E_n(i, j) = -\frac{1}{\log_{10}(w \times w)} \sum_{m=i-w/2}^{i+w/2} \sum_{n=j-w/2}^{j+w/2} \left(\psi_w(m, n) \times \log_{10}(\psi_w(m, n))\right) \tag{18}$$

$$\psi_w(i, j) = \frac{E_\mu(i, j)}{\sum_{m=i-w/2}^{i+w/2} \sum_{n=j-w/2}^{j+w/2} E_\mu(m, n)} \tag{19}$$

$$E_\mu(i, j) = \mu(i, j) \times f_\mu(i, j) \times e_\mu(i, j). \tag{20}$$

The fuzzy entropy, $En(i, j)$, is calculated and used to evaluate the uniformity degree of the local region. The basic idea to determine the amplification exponent constant $k(i, j)$ is that, if $En(i, j)$ is low, it implies that the fuzzy membership of the region varies sharply and the degree of enhancement should be high; therefore, the amplification exponent constant $k(i, j)$ should be small. On the other hand, if $En(i, j)$ is high, the fuzzy membership varies slowly and $k(i, j)$ should be large.

Determine the minimal and maximal amplification constants

If we define the intensity difference between the intensities of a central area and the overall image as ΔL and the overall image intensity as L, the ratio

between the two is called the Weber ratio, W (Gonzalez and Woods 2002):

$$W = \frac{\Delta L}{L}. \tag{21}$$

If a region differs in intensity from its surroundings by less than 2% (Wu et al. 1992; Gonzalez and Woods 2002), it is indistinguishable to the human eye. To increase the image contrast over the Weber ratio and accomplish the enhancement task, the contrast ratio $C_\mu(i, j)$, which is less than 2%, should be transformed to $C'_\mu(i, j)$ that is greater than 2%. The aim of selecting $k_{\max}$ and $k_{\min}$ is to increase image contrast above the threshold. Therefore, we define r = 0.02 as the Weber ratio.

The determination of the minimal and maximal amplification constants, $k_{\min}$ and $k_{\max}$, should relate to the contrast of the original image. At first, the local contrast of the original image is computed and then the contrast level of the entire original image is evaluated. The method to determine $k_{\min}$ and $k_{\max}$ is below.

The local contrast of the original image is:

$$C(i,j) = \left|g(i, j) - \bar{g}_s(i, j)\right| / \left|g(i, j) + \bar{g}_s(i, j)\right| \tag{22}$$

$$\bar{g}_s(i, j) = \frac{1}{s \times s} \sum_{m=i-(s-1)/2}^{i+(s-1)/2} \sum_{n=j-(s-1)/2}^{j+(s-1)/2} g(m, n), \tag{23}$$

where $C(i, j)$ is the local contrast of pixel (i, j) and $\bar{g}_s(i, j)$ is the local mean of the grey levels in the window with size $s \times s$, centered at pixel (i, j).

The mean value of the contrast is:

$$\overline{C}_R = \frac{1}{M} \sum_{(i,j)\in G(R)}^{0\le i\le H-1} \sum_{C(i,j)<R}^{0\le j\le W-1} C(i, j), \tag{24}$$

where H and W are the height and width of the image, $G(R)$ is the region having contrast values smaller than R, M is the number of pixels in this region and $\bar{C}_R$ is the mean contrast value of this region, $R\epsilon(0.1)$. How to determine R is discussed below.

Determine the maximal and minimal amplification constants

The maximal and minimal amplification exponent constants are determined as follows:

$$k_{\max} = \frac{\log R}{\log \bar{C}_R} \tag{25}$$

$$k_{\min} = \frac{\log R}{\log C_{\min}}, \tag{26}$$

where $C_{\min}$ is the minimal value of the contrasts.

The local amplification exponent constant is:

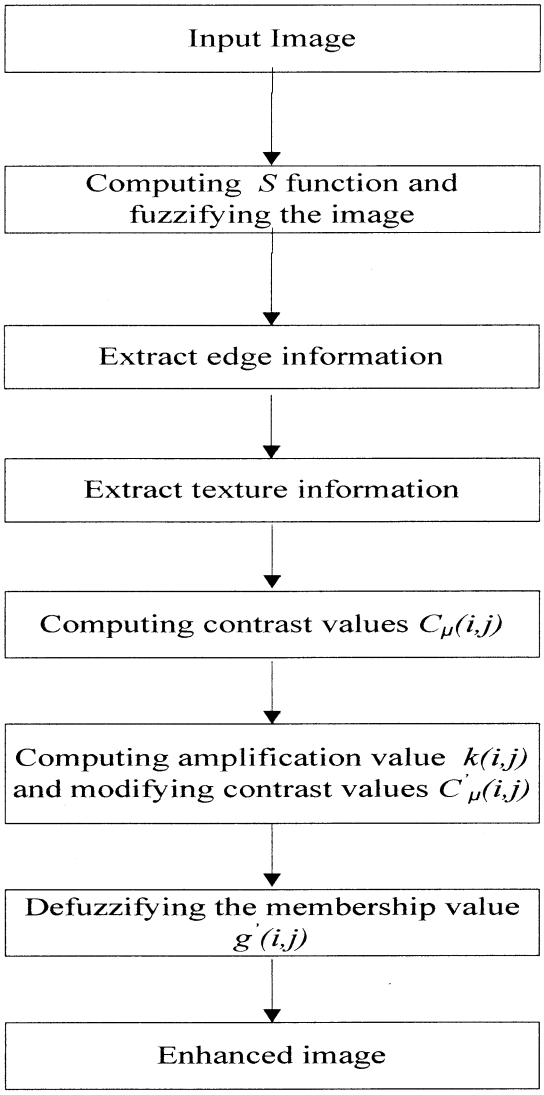

Fig. 2. The flow-chart of the proposed algorithm.

$$k(i, j) = k_{\min} + \frac{\left(En(i, j) - En_{\min}\right) \times \left(k_{\max} - k_{\min}\right)}{En_{\max} - En_{\min}}, \tag{27}$$

where $En_{\min}$ and $En_{\max}$ are the minimal and maximal local fuzzy entropies, respectively.

$$En_{\min} = \min_{i,j}\{En(i, j)\} \tag{27a}$$

and

$$En_{\max} = \max_{i,j}\{En(i, j)\}. \tag{27b}$$

All steps of the algorithm are summarized and shown in a flow-chart in Fig. 2.

Table 1. The parameters for the images

Image	w size	s size	k_{min}	k_{max}
Fig. 3	5 × 5	3 × 3	0.4299	0.8473
Fig. 4	5 × 5	3 × 3	0.4023	0.8528
Fig. 5	5 × 5	3 × 3	0.4700	0.8385
Fig. 6	5 × 5	3 × 3	0.4472	0.8505
Fig. 7	5 × 5	3 × 3	0.4229	0.8634

EXPERIMENTAL RESULTS

The breast US images used in the experiments were provided by the Second Affiliated Hospital of Harbin Medical University, Harbin, China. The images were collected by using a Vivid 7 (GE, Horten, Norway) with a 5- to 14-MHz linear probe and were captured directly from the video signals. The database consisted of a total of 86 images of 49 cases and each single lesion is in one image. Of the 49 cases, 14 were benign solid lesions (30 images) and 35 were malignant solid lesions (56 images). For every patient, 1 to 10 images (2 to 5 images on average) were obtained. The length diameter of most masses was 3 to 4 cm and transverse diameter was 5 to 6 cm. The maximum depth of the masses was 7.0 cm and the minimum depth was 2.0 cm. The average number of pixels of the images was 720 × 576. All lesions were confirmed by biopsy or operation and the tumors were outlined by a radiologist according to the biopsy results.

The program was executed on a single central processing unit Intel Pentium IV 1.7-GHz, 256-MB random access memory personal computer. The average execution time was 3.5 s per image.

Here, we just present a few of the experimental results to demonstrate the performance of the proposed method. The parameters of the examples are listed in Table 1.

Figures 3a to 7a are the original images and Figs. 3b to 7 b are the results obtained by using the proposed method. The mass's features, such as shape, edge and echo inside, are important criteria to distinguish between malignancy and benign tumors. After enhancement, the lesion features were significantly improved.

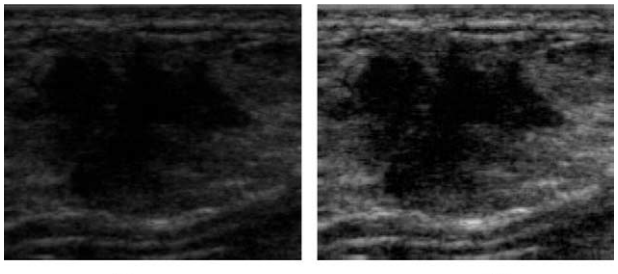

(a) (b)

Fig. 3. Central compact mass; (a) original image, (b) image enhanced by the proposed method.

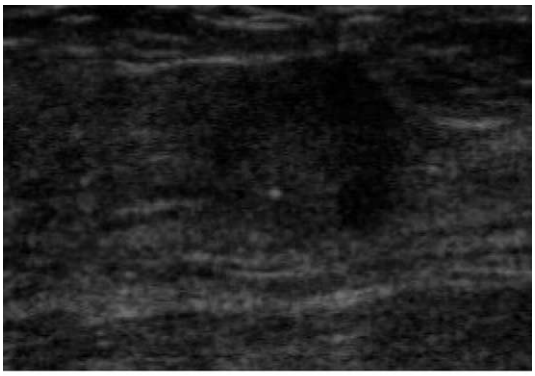

(a)

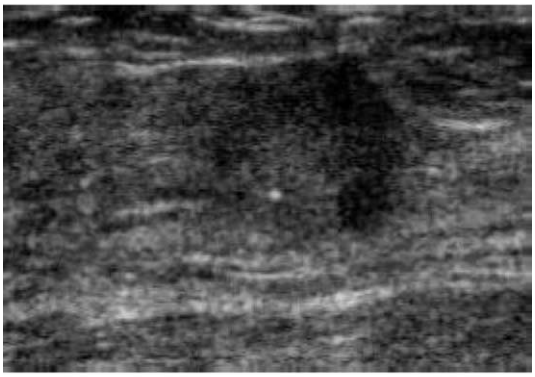

(b)

Fig. 4. Ill-defined border of mass; (a) original image, (b) image enhanced by the proposed method.

Figure 3a has a compact mass at the center of the image. The mass echo and the intensity are very low and the mass is hard to distinguish from the background. In Fig. 3b, the mass becomes clearer and easier to detect and the shape and edge can be better extracted.

In Fig. 4a, the ill-defined border of the mass is almost invisible and not connected, especially the left border and lower border. After applying the proposed method, the border is much clearer and the mass is more distinct.

Figure 5a has a loose cluster of microcalcifications at the center of the mass. In Fig. 5b, those tiny spots become brighter and microcalcifications are more distinct. At the same time, the glandular tissue on the upper area is not overenhanced.

Figure 6a displays a different type of mass, which has a well-circumscribed border. The mass has a low echo inside, the intensity inside the mass is very low and the details cannot be seen clearly. After enhancement,

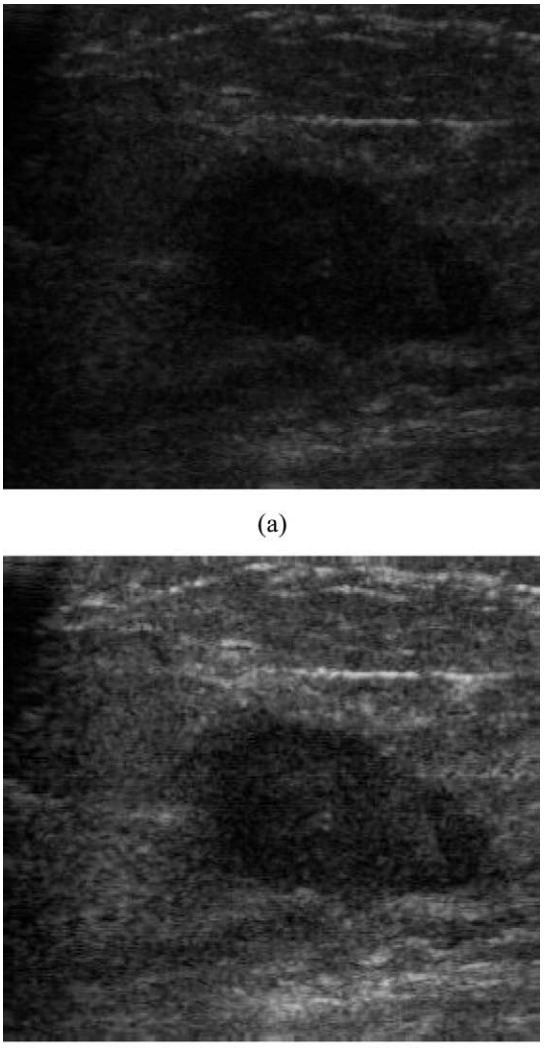

Fig. 5. Loose cluster of microcalcifications; (a) original image, (b) image enhanced by the proposed method.

not only is the boundary of the mass considerably improved, but also the structure inside the mass is well enhanced.

In Fig. 7a, the mass has a blurry edge and the inside structure cannot be seen clearly. The difference between the bottom of the mass and other tissues is very small and it cannot be perceived. In the enhanced image, the bright spots in the lower area are enhanced correctly and can be distinguished easily.

Compared with the histogram equalization method, Fig. 8a shows the original image, Fig, 8b shows the image enhanced by the proposed approach, and Fig. 8c shows the image enhanced by the histogram equalization method, which is very noisy and overenhanced. Figures 9a to c demonstrate the similar results.

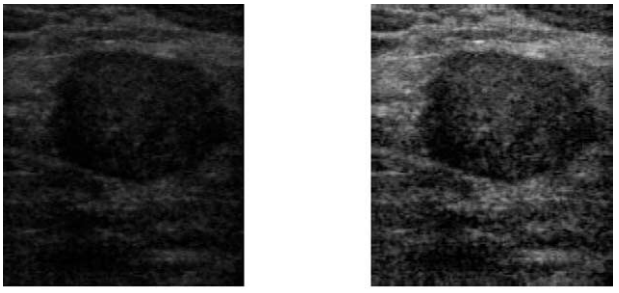

Fig. 6. Mass with well-circumscribed border; (a) original image, (b) image enhanced by the proposed method.

The experiments have shown that the proposed approach can significantly enhance the contours and the fine details of US images and that the enhanced images can be processed further to detect the masses and microcalcifications with high accuracy. The algorithm was applied to clinical diagnosis and the algorithm was evaluated using the receiver operating characteristic (ROC)

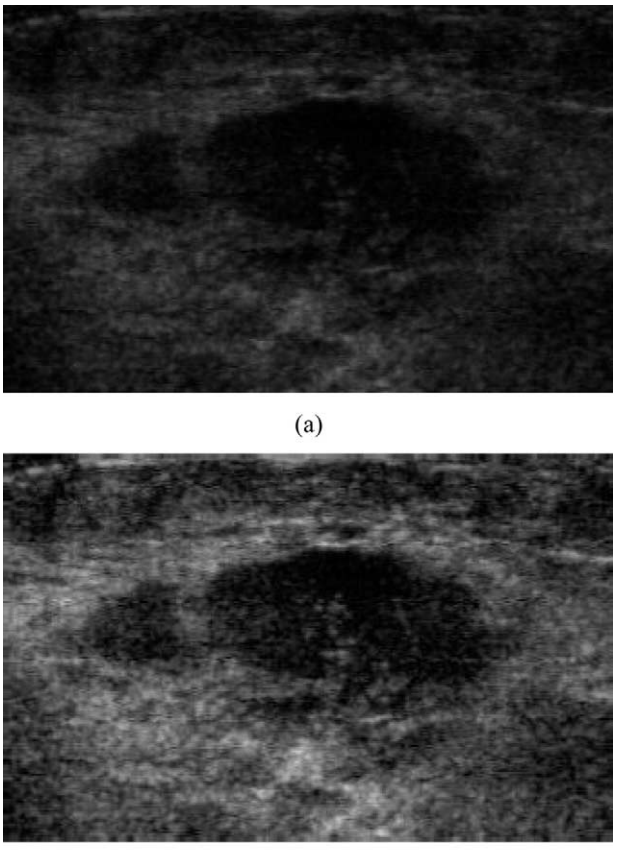

Fig. 7. Mass with blurry edge; (a) original image, (b) image enhanced by the proposed method.

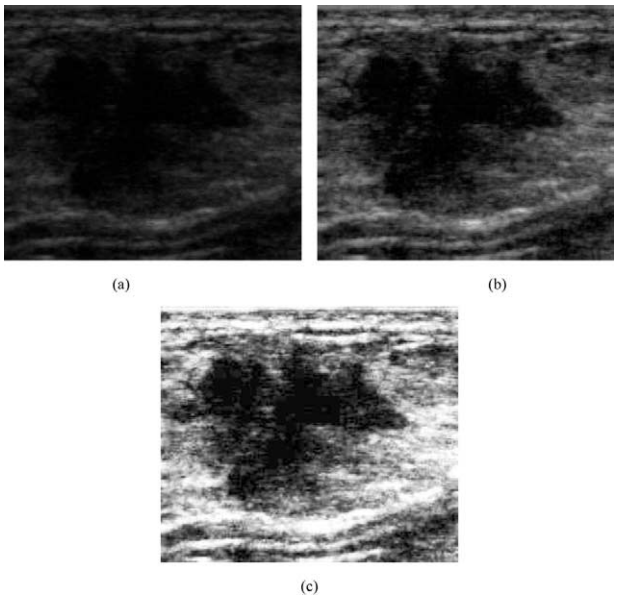

Fig. 8. Comparison with histogram equalization; (a) original image, (b) image enhanced by the proposed method, (c) and enhanced by histogram equalization.

curve (Tian et al. 2005). The results show that the breast lesions that can be diagnosed definitely increased from 29 cases of the original images (malignant 22 cases and benign 7 cases) to 35 cases of the enhanced images (malignant 26 cases and benign 9 cases). At a different cut-off value, the sensitivity and specificity of ultrasonologist diagnosis on the original and enhanced images are, first, when the false-positive rate was 14.3%, the sensitivity of the enhanced images was improved from 80.6% to 82.9%, the positive predictive value (PPV) increased from 93.3% to 93.5% and the negative predictive value (NPV) from 63.2% to 66.7%. When the false-positive rate was 35.7%, the sensitivity of the enhanced images improved from 88.6% to 94.3%, the positive predictive value increased from 86.1% to 91.3% and the negative predictive value from 69.2% to 73.3%. The results of definite diagnosis after enhancement were significantly better than those before enhancement.

From the ROC curve, as shown in Fig. 10, we can conclude that the ROC curve of ultrasonologist diagnosis on the enhanced images was more convex than that on the original images. This implies that it has a higher diagnostic value. For the original images, $A_1 = 0.87$ and its 95% credible interval was [0.756, 0.985]; and, for the enhanced images, A_2 and its 95% credible interval was [0.795, 1.003]. From this, we can also conclude that the enhanced images can improve the accuracy of the diagnosis. The chi-square test was also used to compare the difference between the diagnosis on the original images and the enhanced images. The value of χ^2 was 4.167 and the value of P was between 0.05 and 0.025.

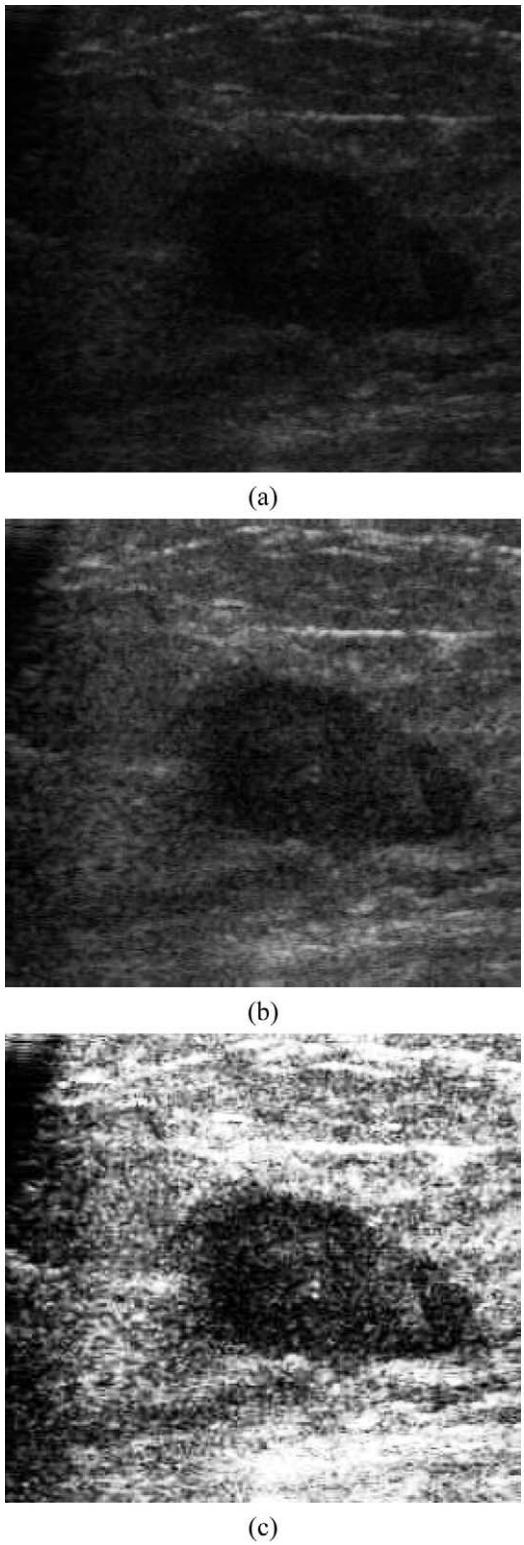

Fig. 9. Comparison with histogram equalization; (a) original image, (b) image enhanced by the proposed method, (c) and enhanced by histogram equalization.

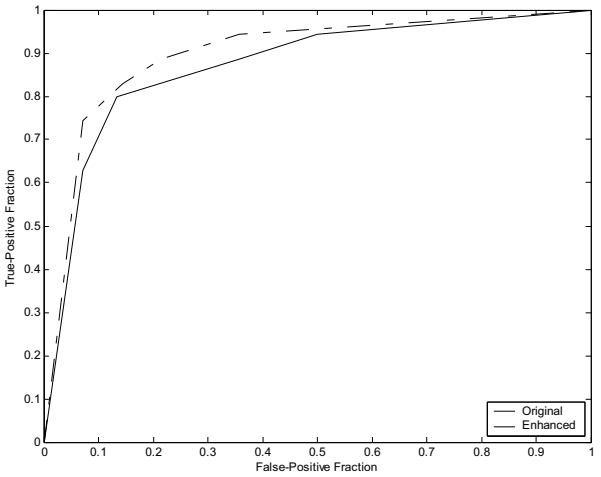

Fig. 10. The ROC curve for experiments (Tian et al. 2005).

The proposed method is very efficient and effective in contrast enhancement: 1. The lesion features of breast US images are better enhanced by the proposed approach and the details are preserved; and 2. the overenhancement and underenhancement are avoided.

CONCLUSIONS

A breast US image-enhancement algorithm based on fuzzy logic and fuzzy entropy was developed. From the experiments, the proposed algorithm makes the details of ROIs much clearer and it has no overenhancement or underenhancement. The good performance is caused by the following factors. 1 The *S* function was used in image fuzzification and the parameters were determined using the maximum entropy principle. Based on the information theory, the fuzzified images contain maximum information. 2. The texture information based on the Laws method was used, which can better describe the textural features of breast US images. 3. Both the local and global information are used to define the local fuzzy contrast. The proposed approach will be useful for breast US image analysis and computer-aided diagnostic systems.

REFERENCES

Abolmaesumi R, Sirouspour MR. Segmentation of prostate contours from ultrasound images. In: Proceedings of IEEE International Conference on speech and signal processing. Vol. 3. Montreal: IEEE, 2004:517–520.

Awad J, Abdel-Galil TK, Salama MMA, et al. Prostate's boundary detection in transrectal ultrasound images using scanning technique. In: IEEE CCECE 2003 Canadian Conference on electrical and computer engineering. Vol. 2. Montreal: IEEE, 2003:1199–1202.

Bassett LW, Ysrael M, Gold RH, Ysrael C. Usefulness of mammography and sonography in women less than 35 years old. Radiography 1991;180:831–835.

Cheng HD, Lui YM, Freimanis RI. A novel approach to microcalcification detection using fuzzy logic technique. IEEE Trans Med Imaging 1998;17(3):442–450.

Dhawan AP, Buelloni G, Gordon R. Enhancement of mammographic features by optimal adaptive neighborhood image processing. IEEE Trans Med Imaging 1986;5:8–15.

Drukker K, Giger ML, Vyborny CJ, Mendelson EB. Computerized detection and classification of cancer on breast ultrasound. Academic Radiol 2004;11(5):526–535.

Farbiz F, Menhaj MB, Motamedi SA, Hagan MT. A new fuzzy logic filter for image enhancement. IEEE Trans Syst Man Cybernet Part B 2000;30(1):110–119.

Gilboa G, Sochen N, Zeevi YY. Image enhancement and denoising by complex diffusion processes. IEEE Trans Patt Anal Machine Intell 2004;26(8):1020–1036.

Gonzalez RC, Woods RE. Digital image processing. 2nd ed. Upper Saddle River, NJ: Prentice Hall, 2002.

Hall EL. Computer image processing and recognition. New York: Academic Press, 1979.

Jackson VP. The role of ultrasound in breast imaging. Radiology 1990;177:305–311.

Joseph YL, Carey EF. Application of artificial neural networks for diagnosis of breast cancer. Proc Cong Evolutionary Comput 1999; 3:1755–1759.

Kapur JN, Sahoo PK, Wong AKC. A new method for grey level picture thresholding using the entropy of the histogram. Comput Vision Graph Image Proc 1985;29:273–285.

Knutzen AM, Gisvold JJ. Likelihood of malignant disease for various categories of mammographically detected, nonpalpable breast lesions. Mayo Clin Proc 1993;68:454–460.

Kopans DB. The positive predictive value of mammography. Am J Roentgenol 1992;158:521–526.

Laine H, Rainio J, Arko H, Tukeva T. Comparison of breast structure and findings by X-ray mammography, ultrasound, cytology and histology: A retrospective study. Eur J Ultrasound 1995;2(2):107–115.

Lanyi M. Diagnosis of breast calcifications. New York: Springer, 1986.

Laws KI. Texture energy measures. In: DARPA Image Understanding Workshop, Los Angeles, CA, 1979. Los Altos: 1979;47–51.

Lee B, Yan JY, Zhuang TG. A dynamic programming based algorithm for optimal edge detection in medical images. In: Shatin NT, ed. Proceedings of the International Workshop on Medical Imaging and Augmented Reality. Hong Kong: 2001:193–198.

Li DD, Shen Y, Liu ZY. A new morphological algorithm for contour extraction on ultrasound image. In: Proceedings of International Conference on Machine Learning and Cybernetics, 2003. vol. 5. Xi'an: 2003:2761–2764.

Li DD, Shen Y, Liu ZY, He P. A new adaptive morphological algorithm for contour extraction on ultrasound image. In: Proceedings of the 21st IEEE Instrumentation and Measurement Technology Conference, 2004. vol. 3: IEEE, 2004:2077–2081.

Mclelland R. Stellate lesions of the breast. Recent Results Cancer Res 1990;119:24–27.

Morrow WM, Paranjape RB, Rangayyan RM, Desautels JEL. Region-based contrast enhancement of mammograms. IEEE Trans Med Imaging 1992;11(3):392–406.

Munteanu C, Rosa A. Gray-scale image enhancement as an automatic process driven by evolution. IEEE Trans Syst Man Cybernet Part B 2004;34(2):1292–1298.

Pal SK, Majumder DKD. Fuzzy mathematical approach to pattern recognition. New York: Wiley, 1986.

Parker JR. Algorithms for image processing and computer vision. New York: John Wiley & Sons, 1997.

Pathak SD, Kim Y. Ultrasound image contrast enhancement via integrating transducer position information. In: Mun, SK, ed. Medical imaging 2000: Image display and visualization, San Diego, CA, USA. 2000:563–572.

Pathak SD, Haynor DR, Kim Y. Edge-guided boundary delineation in prostate ultrasound images. IEEE Trans Med Imaging 2000;19(12): 1211–1219.

Rangayyan RM, Rguyen HN. Pixel-independent image processing techniques for enhancement of features in mammograms. In: Proceedings of the IEEE Engineering Medical Biology Conference. Fort Worth: IEEE, 1986:1113–1117.

Sahoo PK, Soltani S, Wong AKC. A survey of thresholding techniques. Comput Vision Graph Image Proc 1998;41:233–260.

Saim HB, Fhong SC, Noor NBM, Wahab JBA. Contrast resolution enhancement based on wavelet shrinkage and gray level mapping technique. Proc TENCON 2000;2:165–170.

Singh S, Bovis K. An evaluation of contrast enhancement techniques for mammographic breast masses. IEEE Trans Inform Technol Biomed 2005;9(1):109–119.

Sivaramakrishna R, Powell KA, Lieber ML, Chilcote WA, Shekhar R. Texture analysis of lesions in breast ultrasound images. Comput Med Imaging Graph 2002;26(5):303–307.

Tian JW, Sun LT, Guo YH, Cheng HD. The clinical value of breast cancer diagnosis based on computed-aided diagnosis. In: Proceedings of the 8th Joint Conference on Information Sciences, Salt Lake City: 2005:737–740.

Tsubai M, Takemura A, Ito M. Morphological operations for ultrasound images by locally variable structuring elements and their analysis of effective parameters. In: Proceedings of the 22nd Annual International Conference of the IEEE. Vol. 4. Chicago, IL: IEEE, 2000:2526–2528.

Wu CM, Chen YC, Hsieh KS. Texture features for classification of ultrasonic liver images. IEEE Trans Med Imaging 1992;11(2):141–152.

Xiao G, Brady JM, Noble JA, Zhang Y. Contrast enhancement and segmentation of ultrasound images—A statistical method. Proc SPIE Med Imaging Image Proc 2000;3979:1116–1125.

Zhou QW, Liu LZ, Zhang DL, Bian ZZ. Denoise and contrast enhancement of ultrasound speckle image based on wavelet. In: Sixth International Conference on Signal Processing. Vol. 2. Beijing, China: 2002:1500–1503.